

Compaction behavior of nonwoven geotextile-reinforced clay

M.-D. Nguyen¹, K.-H. Yang² and W. M. Yalew³

¹Assistant Professor, Department of Soil Mechanics and Foundations, University of Technology and Education, Ho Chi Minh City, Vietnam, E-mail: ducnm@hcmute.edu.vn (corresponding author)

²Professor, Department of Civil Engineering, National Taiwan University (NTU), Taipei, Taiwan E-mail: khyang@ntu.edu.tw

³Lecturer, Faculty of Civil and Water Resources Engineering, Bahir Dar University, P.O. Box 26, Bahir Dar, Ethiopia, E-mail: wubmngst@gmail.com

Received 02 January 2019, revised 02 July 2019, accepted 22 August 2019, published 25 November 2019

ABSTRACT: This paper presents a series of compaction tests for investigating the compaction behavior of nonwoven geotextile-reinforced clay and the effects of permeable geotextiles on improvements in the density of reinforced clay. Specimens were compacted by varying the compaction energy, number of geotextile layers and compaction lift thickness. The compaction test results were analyzed from the pure soil between the reinforcement layers without including the thickness of embedded reinforcement layers. The test results indicate that the density of reinforced clay increased with the number of geotextile layers without significant changes in the optimum moisture content (OMC). Due to the reinforcing effect, up to 50% standard compaction energy could be saved when compacting the reinforced clay to achieve the same density as that of unreinforced clay. When the degree of saturation of soil was over 90%, water absorption in the reinforcement layers increased sharply, improving the effects of permeable geotextile on dissipation of the pore water pressure in the soil of the reinforced specimens. When the water content of reinforced soil was 6.7% higher than the OMC, the water absorption of the reinforcement layers reduced the void ratio of reinforced specimens under standard compaction energy by 4.5–5.5%.

KEYWORDS: Geosynthetics, Reinforced clay, Compaction, Void ratio

REFERENCE: Nguyen, M.-D., Yang, K.-H. and Yalew, W. M. (2020). Compaction behavior of nonwoven geotextile-reinforced clay. *Geosynthetics International*, 27, No. 1, 16–33. [<https://doi.org/10.1680/jgein.19.00053>]

1. INTRODUCTION

Geosynthetic reinforced soil (GRS) structures are widely used as a green alternative to reinforced concrete structures. To ensure the effective performance of GRS structures, current design guidelines (Elias *et al.* 2001; AASHTO 2002; Berg *et al.* 2009; NCMA 2010) specify the use of free-draining granular materials as backfill materials within a reinforced zone and preclude the use of fine-grained materials. However, in most construction cases, the specified materials are not available and must be imported from other locations; this significantly increases the construction cost of GRS structures.

The clay excavated from the Mekong Delta in Vietnam is a cheap and easily available material for use as backfill soil in GRS structures. However, soft riverbed clay is unsuitable as a backfill material because of its low shear strength, high void ratio and impermeability. The reduction in soil shear strength and soil-reinforcement interface strength from excess pore water pressure

during construction or after rainfall is the main concern over using cohesive soil as the backfill soil for GRS structures.

To improve the mechanical properties of clay and minimize excess pore water pressure in the backfill, one approach is to combine compaction with permeable geosynthetic layers. The use of nonwoven geotextile in the construction of full-scale test GRS walls with marginal backfill has been reported (Tatsuoka and Yamauchi 1986; Portelinha *et al.* 2013). The enhancement of the internal stability of the GRS structures can be achieved through the dissipation of pore water pressures in the soil mass due to the high permeability of nonwoven geotextile reinforcements (Fourie and Fabian 1987; Ling *et al.* 1993; Zornberg *et al.* 1998; Tan *et al.* 2001; Iryo and Rowe 2005; Noorzad and Mirmoradi 2010; Raisinghani and Viswanadham 2010). Although the performance and behavior of reinforced soil have been extensively studied, the compaction behavior of reinforced soil during construction has not yet been fully investigated due to the

complex interaction between soil and reinforcement materials.

Soil compaction is a method used to mechanically enhance the density of unsaturated soil by reducing the air volume without changing the water volume in the pore space. Compaction is aimed at increasing soil strength and stiffness by reducing the compressibility and permeability of the soil mass by reducing its porosity (Lambe and Whitman 1969; Rollings and Rollings 1996; Holtz *et al.* 2010).

The compaction of unsaturated soil induces changes in the pore water pressure, microscopic soil structure, and degree of saturation. Gupta *et al.* (1989) observed a correlation between changes in microscopic soil structure and the degree of saturation with the development of negative pore water pressure during compaction. Laboratory measurements showed that the pore water pressure increased and then decreased with an increase in applied mechanical load. The minimum pore water pressure (indicating shearing or plastic deformation of aggregates in the soil structure) occurs for soils with a degree of saturation of approximately 40–60% (Gupta *et al.* 1989). Lins and Sandroni (1994) measured the development of pore water pressure in unsaturated compacted soil with constant water content subjected to isotropic compression and concluded that positive pore water pressure is unlikely to occur for soils with a degree of saturation below the corresponding value at the optimum water content, w_{opt} . Li *et al.* (2011) investigated changes in the pore water pressure of clay during dynamic compaction in BinDei Highway, China, and observed the occurrence of excess pore water pressure at shallow depths, noting that the unsaturated clay required more time to dissipate at greater depths.

Related to the influence of compaction energy on the compaction behavior of clay, an increase in the compaction energy induced an increase in the maximum dry unit weight, γ_{d-max} , and a decrease in w_{opt} (Blotz *et al.* 1998; Gurtug and Sridharan 2004; Tatsuoka and Correia 2016). Tatsuoka and Correia (2016) also investigated the influence of the degree of saturation on the compaction behavior of clayey soil. The optimum degree of saturation $(S_r)_{opt}$ is defined as S_r , where γ_{d-max} is obtained for a given compaction energy level and a given soil type. The experimental results showed that $(S_r)_{opt}$ and the relationship between the true degree of compaction γ_d/γ_{d-max} and $S_r - (S_r)_{opt}$ of compacted soil are insensitive to variations in the compaction energy and soil type.

Further, compaction lift thickness significantly influences soil compaction behavior. Turnbull and Foster (1956) evaluated the effect of lift thickness on the density gradient versus depth in lean clay (CL). They found that the dry density gradient is steeper for a 0.3 m thickness than for a 0.6 m lift thickness for compacted soils with water content higher than the optimum moisture content (i.e. the wet side of optimum). D'Appolonia *et al.* (1969) evaluated the effective depth of influence of a vibratory roller (diameter: 1.2 m, width: 2 m, pressure: 86 MPa) in coarse-graded soil. They suggested that suitable lift thickness could be selected by

taking the density profile of a thick lift compacted using a given compactor after five passes.

Apart from unreinforced soil, the water absorption of reinforcement during compaction induces changes in the water content of compacted reinforced soil. Studies have reported different influences of reinforcement on compaction behavior. Studies on the compaction of clay reinforced by fibers such as polypropylene or coir showed that the compaction characteristics of unreinforced and reinforced clay are similar; however, an increase in fiber content induces an increase in maximum dry unit weight and a decrease in optimum moisture content w_{opt} (Maher and Ho 1994; Nataraj and McManis 1997; Plé and Lê 2012; Devdatt *et al.* 2015). Leshchinsky (2000) and Jiang *et al.* (2016) investigated the influence of secondary reinforcement, additional reinforcement layers between primary reinforcement layers, on the performance of GRS walls. Their studies suggested that the inclusion of secondary reinforcement has the beneficial effect of improvement in compaction behind the wall facing. By contrast, the opposite compaction behaviors of geotextile-reinforced clay were also reported (Chegenizadeh and Nikraz 2011; Chaple and Dhattrak 2013; Mirzababaei *et al.* 2013; Tilak *et al.* 2015; Soundara and Senthil 2015). Parihar *et al.* (2015) studied the compaction of clay reinforced by woven and nonwoven geotextiles and concluded that geotextile layers reduce w_{opt} and change the maximum dry unit weight (an increase or decrease depending on the type of geotextile and its inclination). Keskin *et al.* (2009) reported that the w_{opt} of reinforced clay is smaller than that of unreinforced clay. However, the maximum dry unit weight of woven and nonwoven geotextile-reinforced specimens is respectively higher and lower than that of unreinforced specimens.

Studies may have provided misleading results on the compaction behavior of reinforced soil, because the behavior may have been evaluated using the overall weight and volume of compacted specimens without deducting the weight and volume of reinforcement. Thus far, limited studies have considered soil alone to evaluate the effects of reinforcement on the compaction behavior of reinforced soil. Indraratna *et al.* (1991) were the first to determine the dry unit weight and water content of soil compacted between fabric layers without considering the overall specimen with geotextiles. A series of compaction tests on nonwoven and woven geotextile-reinforced clay revealed a significant increase in dry density and decrease in porosity; these were explained by the enhanced dissipation of excess pore water pressure and the high air permeability of nonwoven geotextiles. Furthermore, the optimum moisture content, w_{opt} , of the fabric-reinforced soil changed only marginally with geotextile spacing.

In light of these observations, this study conducted a series of compaction tests of clay reinforced by a nonwoven geotextile by varying the lift thickness, compaction energy, and number of reinforcement layers. The objectives of this study are (1) to estimate the improvement in the density and void ratio of pure soil between reinforcement layers in the reinforced clay through compaction tests under different conditions,

(2) to quantify the compaction energy saving due to the effect of reinforcement on enhancing the density of reinforced clay, (3) to assess the mechanical compaction behavior of reinforced clay using the correlation between the water content of reinforcement layers and the degree of saturation of reinforced specimens, and (4) to study the effect of the water absorption of permeable geotextile on improving the density of reinforced clay. The study results provide useful information for using nonwoven geotextiles to effectively improve the compaction behavior of riverbed clay, which could replace sandy soil as cheap backfill for embankment constructions in local areas.

2. EXPERIMENTAL PROGRAM

A total of 110 standard and modified laboratory compaction tests were performed to investigate the compaction behavior of cohesive soil with and without reinforcement. The test variables involve compaction energy, water content, number of geotextile layers, and compaction layers. After compaction tests were conducted, the soil unit weight and the water content of reinforcement layers was measured using a high-precision water content determination method.

2.1. Test materials

2.1.1. Clay

KienGiang clay was excavated from the riverbed of Cai Lon River in the Mekong Delta, Vietnam. Figure 1 shows the grain-size distribution of clay determined from a sieve and hydrometer test (ASTM D 422). The soil is classified as high plastic inorganic silt (MH) by the Unified Soil Classification System (USCS), which has specific gravity (G_s) of 2.75, liquid limit (LL) of 91.5, plastic limit (PL) of 44.9, and plasticity index (PI) of 46.6. The optimum water content and maximum dry unit weight determined from standard Proctor compaction (ASTM D 698) are $w_{opt} = 31.5\%$ and $\gamma_{d,max} = 13.21 \text{ kN/m}^3$, respectively. The saturated hydraulic conductivity of the soil at the maximum density state estimated using Terzaghi's 1D consolidation theory is $k_{sat} = 1.18 \times 10^{-10} \text{ m/s}$, as shown in Table 1.

2.1.2. Geotextile

A commercially available needle-punched polyethylene terephthalate (PET) nonwoven geotextile was used.

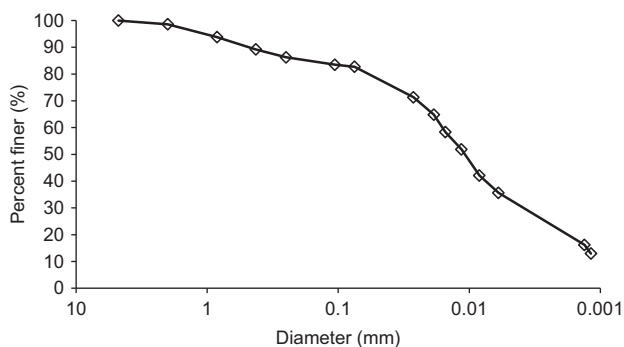


Figure 1. Grain size distribution of KienGiang clay

Table 1. Properties of KienGiang clay

| Property | Value |
|--|-------|
| Unified Soil Classification System | MH |
| Plastic limit, PL (%) | 44.9 |
| Plastic index, PI (%) | 46.6 |
| Specific gravity, G_s | 2.75 |
| Total unit weight, γ (kN/m ³) | 16.13 |
| Void ratio, e | 1.60 |
| Natural water content of soil, w_{soil} (%) | 57.4 |
| Degree of saturation, S_r (%) | 96.6 |
| Liquid limit, LL (%) | 91.5 |
| Optimum water content, w_{opt} (%) | 31.5 |
| Maximum dry unit weight, $\gamma_{d,max}$ (kN/m ³) | 13.21 |

The nonwoven geotextile was selected due to its high permeability, because this significantly reduces pore water pressure in reinforced samples during compaction. Table 2 summarizes the properties of the tested nonwoven geotextile. Based on the permittivity test (ASTM D 4491), the geotextile has permittivity of $\psi = 1.96 \text{ s}^{-1}$ and corresponding cross-plane permeability of $k = 3.5 \times 10^{-3} \text{ m/s}$, which is several orders of magnitude higher than the permeability of the clay used in this study. The load-elongation behavior of the reinforcement was tested by wide-width (ASTM D 4595) and biaxial tensile tests (Nguyen *et al.* 2013) in the longitudinal and transverse directions as well as by a puncture-strength test (Yang *et al.* 2016). The test results revealed the anisotropic tensile behavior of the geotextile.

2.2. Specimen preparation

A natural clay sample excavated from the riverbed in the form of wet bulk was placed in an oven (temperature was set at less than 60°C) for a minimum of 24 h and then crushed and ground into a dry powder in a mortar. Moist soil specimens were prepared by mixing different quantities of powder and water corresponding to the desired water content, with the mixture being placed in a plastic bag within a temperature-controlled chamber and sealed for a minimum of 2 days to ensure a uniform distribution of moisture within the soil mass.

2.3. Testing program

A total of 50 compaction tests were performed on the unreinforced clay under different water content values, compaction energies, and compaction layers. Regarding reinforced clay specimens, 60 compaction tests were conducted by varying the water content values, number of reinforcement layers, and compaction energies.

The variation of water content and compaction energy of all specimens (i.e. unreinforced and reinforced specimens) was 20–45% and 600–2700 kJ/m³, respectively. The specimens were compacted using a mold with a 101.4 mm diameter and height of 116.6 mm. The number of blows per compaction layer and type of rammer used depended on the compaction energies. Two types of rammer were used: a Proctor rammer (i.e. 24.5 N drop from 305 mm)

Table 2 Physical and hydraulic properties of nonwoven geotextile

| Property | Value | | |
|---------------------------------|--|--|--|
| Fabrication process | Needle-punched PET nonwoven geotextile | | |
| Mass (g/m ²) | 200 | | |
| Thickness (mm) | 1.78 | | |
| Apparent opening size (mm) | 0.11 | | |
| Permittivity (s ⁻¹) | 1.96 | | |
| Cross-plane permeability (m/s) | 3.5 × 10 ⁻³ | | |

| Direction | Ultimate strength (kN/m) | Failure strain (%) | Secant stiffness @ peak value (kN/m) |
|-------------------------|--------------------------|--------------------|--------------------------------------|
| Wide-width tensile test | | | |
| Longitudinal | 9.28 | 84.1 | 11.03 |
| Transverse | 7.08 | 117.8 | 6.01 |
| Biaxial tensile test | | | |
| Longitudinal | 7.53 | 20.3 | 37.09 |
| Transverse | 5.91 | 24.3 | 24.32 |
| Puncture strength test | | | |
| Axisymmetric | 12.3 | 65.6 | 18.75 |

and a modified Proctor rammer (i.e. 44.48 N drop from 457.2 mm), as listed in Table 3.

For unreinforced specimens, clay specimens were compacted in two, three, five, and six layers (Figure 2a) to investigate the influence of compaction lift on the compaction behavior of clay. The amount of soil for each compaction layer was evaluated using several trial compaction tests. The total amount of soil used should be such that the last compacted layer slightly extends into the collar but not more than ~6 mm above the top of the mold, as required in ASTM D 698 and ASTM D 1557. Before the collar was removed to trim the compaction specimen, the soil adjacent to the collar was trimmed to loosen it from the collar and to avoid disrupting the soil below the top of the mold. A knife was used to trim the compacted specimen even with the top of the mold. Any holes in the top surface were filled with unused soil and pressed in with fingers; then, a straight edge was scraped across the top of the mold. After the specimens were compacted, their moisture weight, W , and the water content of the soil, w , were measured (following ASTM D 2216). The dry unit weight of unreinforced specimens, γ_{d-unre} , was evaluated as

$$\gamma_{d-unre} = \frac{W}{(1+w)V} \quad (1)$$

where V = mold volume.

The reinforced specimens were compacted in six compaction layers and stabilized with one, two, and five reinforcement layers (Figure 2b). After each soil layer was compacted and leveled, the soil surface was scarified before a 101.6 mm-diameter dry geotextile layer was placed horizontally on the roughed surface. The amount of soil required for the next layer was then poured and compacted. The process for completing the surface of reinforced specimens was similar to that for unreinforced specimens. The moisture weight of the reinforced specimen, W_{re} and water content of the soil, w , was measured in the reinforced specimens.

Although the unreinforced and reinforced specimens were compacted using clay prepared with the same water content, it was observed that the water content in reinforced specimens was slightly lower than that in unreinforced specimens due to water absorption by the reinforcement layers (considering the same reduction in the water content of unreinforced and reinforced soil due to evaporation during compaction). Besides, the distribution of the water content of soil in reinforced specimens seemed nonuniform. The water content of soil adjacent to the reinforcement layers was lower than the original water content due to water drainage; by contrast, higher water content was found in the soil far from the reinforcement layers. As a result, the water content of reinforced specimens should be evaluated as the average value for

Table 3. Compaction method and energies

| Compaction energies, E , (kJ/m ³) | Compaction methods | Total number of blows |
|---|--|-----------------------|
| 600 | Standard compaction energy 24.5 N rammer dropped from a height of 30.5 cm | 75 |
| 960 | Modified compaction energy 24.5 N rammer dropped from a height of 30.5 cm | 120 |
| 1920 | Modified compaction energy 24.5 N rammer dropped from a height of 30.5 cm | 240 |
| 2700 | Modified compaction energy 44.5 N rammer dropped from a height of 45.7 cm | 125 |

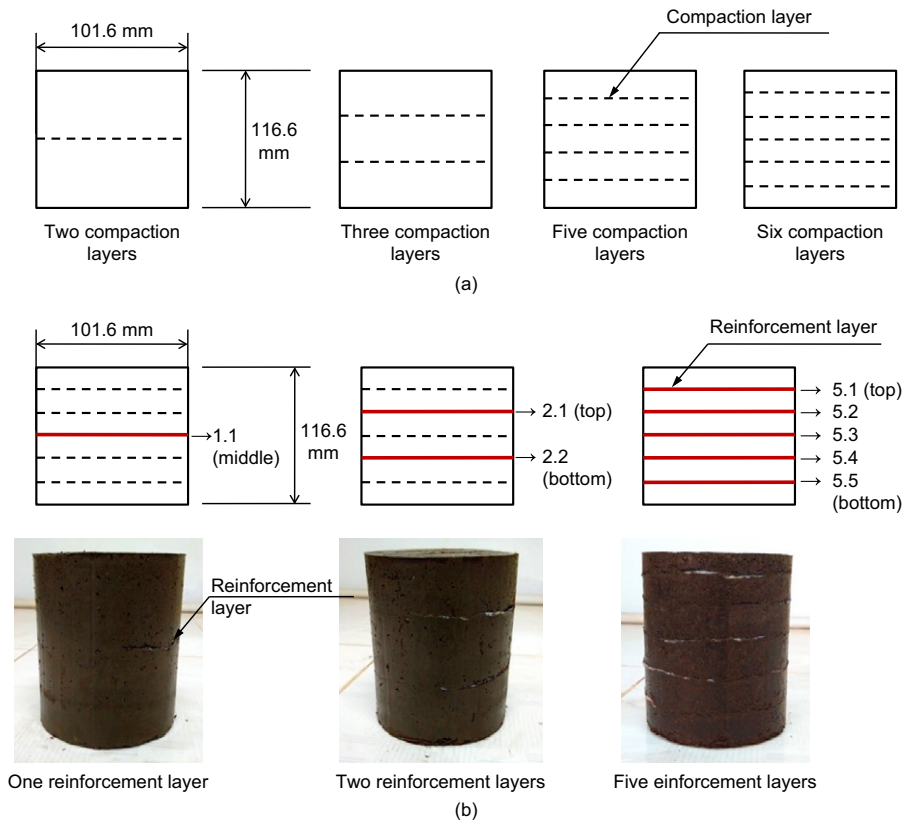


Figure 2. Arrangement of compaction layers and reinforcement layers in (a) unreinforced specimens and (b) reinforced specimens

the overall specimens rather than the measured water content for several extracted soil samples.

The water content reduction Δw due to water absorption by reinforcement layers in the reinforced specimens was evaluated as

$$\Delta w = \frac{w_{geo} W_{d-geo}}{W_{d-soil}} \quad (2)$$

in which W_{d-geo} and w_{geo} are the dry weight and water content of geotextile layers in reinforced soil, respectively. The first parameter (i.e. W_{d-geo}) was measured before compaction tests. The second parameter (i.e. w_{geo}) was estimated based on the dry and moisture weight of reinforcement layers retrieved after compaction tests (as discussed in the next section).

W_{d-soil} is the total weight of dry soil in reinforced soil specimens after compaction. As the soil of unreinforced and reinforced specimens was prepared with the same water content, considering the same reduction of water content in unreinforced and reinforced soil due to evaporation during compaction, the total weight of dry soil in reinforced specimens was determined as

$$W_{d-soil} = \frac{W_{re} - W_{d-geo}}{1 + w} \quad (3)$$

where W_{re} is the moisture weight of reinforced specimens.

Figure 3 shows the calculated water content reduction; Δw was very small ($\Delta w < 0.3\%$). The higher the number of reinforcement layers and the higher the water content of the soil, the greater the amount of water from the soil that was infiltrated into the geotextile layers. In addition, the

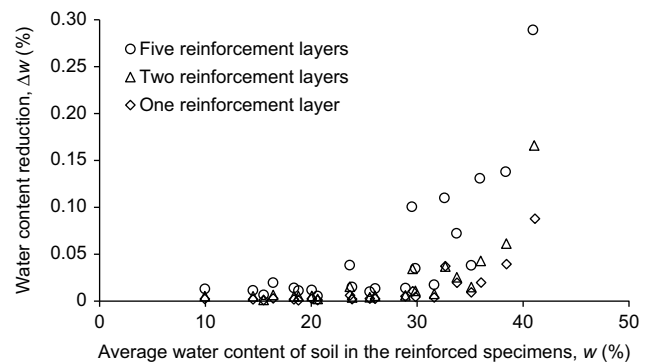


Figure 3. Variation of water content reduction with the average water content of soil in reinforced specimens

water absorption in the geotextile layers did not greatly influence the water content of the reinforced specimens due to the low percentage of geotextiles in the reinforced soil specimens (i.e. 0.1–0.6% in weight).

The dry unit weight of the soil in the reinforced specimen, γ_{d-re} , was determined from the dry weight and volume of the soil only after deducting the dry weight and volume of reinforcement layers from the reinforced specimens. Indraratna *et al.* (1991) were the first to evaluate actual soil compaction by considering the dry unit weight for pure soil compacted between geotextile layers in lieu of the overall specimens with the reinforcement. As a result, the problems caused by the total thickness of the geotextile in evaluating the dry density of soil in reinforced specimens were avoided.

$$\gamma_{d-re} = \frac{W_{d-soil}}{V - V_{geo}} \quad (4)$$

where V_{geo} = total volume of all reinforcement layers, which was evaluated as

$$V_{geo} = \frac{\pi}{4} d^2 \sum_{i=1}^{n_r} t_i \quad (5)$$

where d is the diameter of the reinforcement layer (101.6 mm); i and n_r are ordinal number and total number of reinforcement layers in reinforced specimens, respectively; and t_i is the actual thickness of reinforcement layer i in compacted specimens.

The actual thickness of the reinforcement layer t_i is reduced significantly compared to the undeformed thickness $t = 1.78$ mm. During compaction, the rammer applies dynamic forces perpendicularly to the planar plane of the geotextile layer through its drops. As a result, the thickness of the geotextile layer decreases as it is compressed under the impact forces and then the elastic deformation recovers after each drop of the rammer. This process is repeated until the compaction process is finished. Subsequently, the geotextile layer is compressed slightly by the overburden pressure of the soil layer above. The method to estimate t_i is discussed in Section 2.5.

2.4. Technique for measuring reinforcement water content

The water content of reinforcement layers was determined using a high-precision water content determination technique. Before the compaction test, geotextile specimens were cut into 101.6 mm-diameter circular discs and oven dried, and their dry weight, W_{d-geo} was measured using a high-precision balance. After the compaction test of reinforced specimens was complete, the reinforcement layers were carefully retrieved from the specimens. Owing to the compaction force, the wet clay and water adhered into the reinforcement layers (Figure 2). The water content of the reinforcement layers was determined as the wet weight of the tested geotextile discs retrieved from the dismantled reinforced specimens (i.e. weight of reinforcement and included soil) immediately after compaction tests and the dry weight of the tested geotextile discs after being oven dried, $W_{w,tested_geo}$ and $W_{d,tested_geo}$, respectively.

$$w_{geo} = w - \frac{(1 + w) W_{d,tested_geo} - W_{w,tested_geo}}{W_{d-geo}} \quad (6)$$

Due to the small difference between the water content of reinforced and unreinforced specimens (less than 0.3%), the water content of the geotextile layers w_{geo} could be evaluated using the water content of unreinforced specimens without inducing a significant error.

2.5. Estimating the actual thickness of the geotextile layer in compacted specimens

The thicknesses of geotextile layers were reduced from their undeformed thicknesses due to the dynamic compaction force and overburden pressure in the compacted

specimens. Due to the difficulty in measuring the actual thickness of geotextile layers in the compacted specimens, this was determined from the upper bound value t_{max} (i.e. maximum thickness value) and lower bound value t_{min} (i.e. minimum thickness value). The upper bound value was the thickness of geotextile layers under the overburden pressure, σ_v , of the soil layer above without any compaction. The lower bound value was the thickness under σ_v after performing the compaction test on geotextile layers alone (without soil). The number of rammer drops onto the reinforcement layer depended on its location and the compaction energy required for the compacted specimen (Figure 2b). The impact force from rammer drops onto the geotextile layers is higher than that onto geotextile layers with soil. This is because the distance that the rammer travels to the reinforcement layers during impact is smaller than that which it travels to the reinforced specimens (for the same potential energy). As a result, the thickness of the geotextile layer compacted without soil was smaller, as expected, than the actual thickness of the geotextile in the compacted specimens.

The overburden pressure acting on a geotextile layer, σ_v is evaluated as

$$\sigma_v = h_{re} \gamma \quad (7)$$

where h_{re} is the depth of the geotextile layer in compacted specimens, and γ is the bulk unit weight of the compacted soil, which varies from 15.1 to 20.7 kN/m³.

The thickness of the geotextile was determined under normal pressure following ISO 9863-1:2016(E) (ISO 2016). Because the range of normal pressure is small (i.e. 0.25–1.75 kPa), a 10 cm-diameter circular presser foot was used (instead of 5 cm, as specified by ISO 9863-1:2016(E) (ISO 2016)) to magnify the compression force. The specified normal pressure was applied for 30 s before measuring the thickness of the geotextile layer. For each level of axial pressure, the mean thickness was evaluated with less than 1% coefficient of variation from the testing results of 10 geotextile specimens.

Figure 4 shows that the average thickness of the geotextile specimens reduced when increasing either the applied normal force or the number of drops of the compaction rammer. The actual thickness of reinforcement layer i in reinforced compacted specimens was determined as the average value of t_{max} and t_{min} .

$$t_i = \frac{t_{max} + t_{min}}{2} \quad (8)$$

The error of the dry unit weight of soil due to the evaluation of t_i was assessed from the standard deviation of the geotextile thickness σ_{ti} .

$$\sigma_{ti} = \frac{t_{max} - t_{min}}{2} \quad (9)$$

From Equations 4 and 5, by considering the thickness of each reinforcement as a variable in the function of dry density of soil in reinforced specimens, γ_{d-re} , and applying the derivation of the function of γ_{d-re} , the error of γ_{d-re} can be presented using the fractional error.

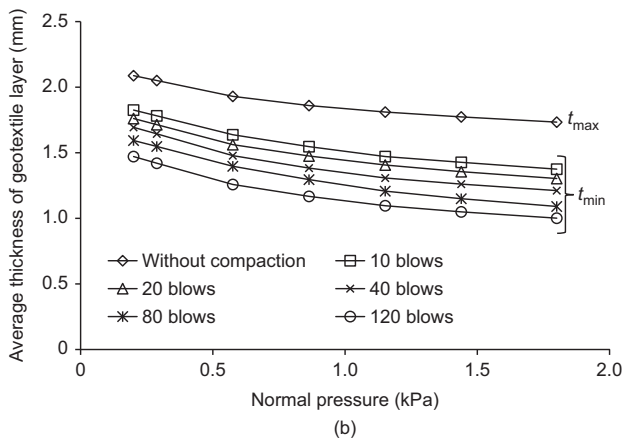
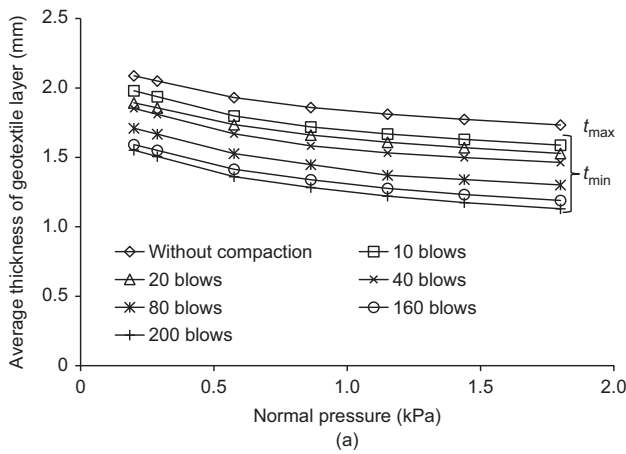


Figure 4. Variation of the average thickness of geotextile layer under different normal pressures and number blows of (a) 24.5 N rammer and (b) 44.5 N rammer

$$\frac{\sigma_{\gamma_{d-re}}}{\gamma_{d-re}} = \frac{\sqrt{\sum_{i=1}^{n_r} \sigma_{t_i}^2}}{H - \sum_{i=1}^{n_r} t_i} \quad (10)$$

The results of fractional error $\sigma_{\gamma_{d-re}}/\gamma_{d-re}$ show that for all cases, the values are less than 0.6%. The error increases for specimens reinforced by a higher number of reinforcement layers (Figure 5). The error analysis showed that the proposed method was applicable for evaluating the thickness of reinforcement layers in reinforced soil after compaction.

3. RESULTS AND DISCUSSION

This section discusses the experimental results from the compaction tests of reinforced and unreinforced clay specimens.

3.1. Influence of lift thickness on the compacted density of clay

Soil samples were compacted in two, three, five, and six layers under the standard compaction energy (i.e. 600 kJ/m³) to evaluate the influence of lift thickness on the dry unit weight of unreinforced clay specimens. The test results shown in Figure 6 revealed that for the same compaction energy, the thickness of each compaction layer insignificantly influenced the optimum water

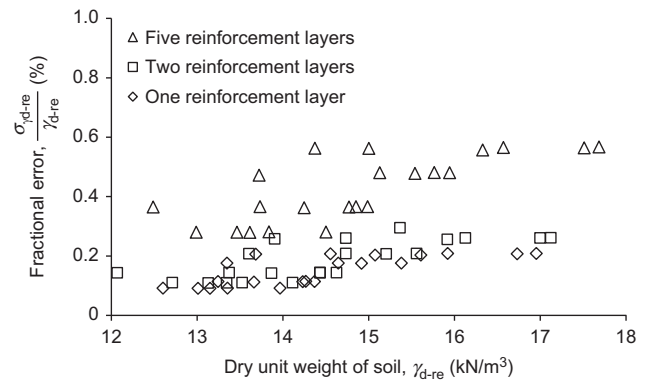


Figure 5. Fractional error with different dry unit weights of soil

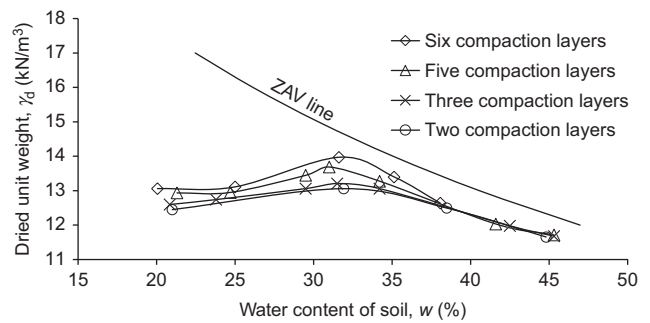


Figure 6. Variation of the dry unit weight of clay specimens when compacting at different water contents and compaction layers

content, OMC ($w_{opt} \approx 31.5\%$), but not their dry density (Figures 6). The higher the number of compaction layers, the higher was the dry unit weight of specimens. Turnbull and Foster (1956) reported a similar finding when evaluating the effect of lift thickness on the density gradient versus depth in a low-plasticity clay (CL).

When specimens were compacted at the dry side of OMC, a significant increase in the dry unit weight of clay specimens was achieved with an increase in the number of compaction layers (i.e. a decrease in lift thickness). By contrast, the increase in dry density was less pronounced for specimens compacted at the wet side of OMC.

The effects of lift thickness on the improvement in the dry unit weight of compacted soil were evaluated using the percentage of dry unit weight difference, %DD_L. This is defined as the difference in percentage difference of dry unit weight between the dry unit weight of soil compacted by n_c compaction layers and two compaction layers, $\gamma_{d-nlayers}$ and $\gamma_{d-2layers}$, respectively.

$$\%DD_L = \frac{\gamma_{d-nlayers} - \gamma_{d-2layers}}{\gamma_{d-2layers}} \times 100\% \quad (11)$$

The lift thickness l was defined as the thickness of each compaction layer (Figure 2)

$$l = \frac{H}{n_c + 1} \quad (12)$$

where H is the total height of the compacted specimen (= 11.66 cm).

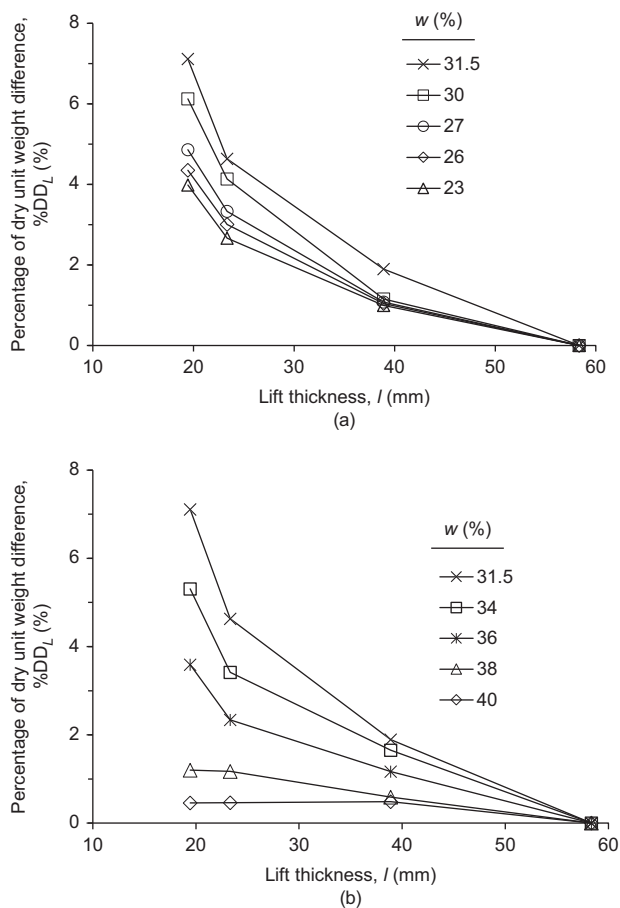


Figure 7. Effects of thickness lift and water content on the percentage of dry unit weight difference (a) specimens compacted on the dry side of OMC; and (b) specimens compacted on the wet side of OMC

Figure 7 shows that the dry unit weight difference increased as the lift thickness *l* was decreased (i.e. as the number of compaction layers was increased). At the optimum water content, the density of the specimen increased up to 7.1% when the lift thickness was reduced from 58.3 to 19.4 mm. In general, the greater the difference in compaction water content from *w*_{opt}, the less the dry density improvement of the samples. However, the compaction behavior of clay specimens on the dry side of OMC was different from that on the wet side of OMC. For a ~10% lower water content than *w*_{opt}, the dry unit weight improvement of specimens compacted at *l* = 19.4 mm was approximately 4%. The dry density of compacted specimens decreased dramatically at a water content higher than *w*_{opt}. At an 8.5% higher water content than *w*_{opt}, less than 1% dry density improvement was observed, even when the lift thickness value was tripled.

3.2. Compaction behavior of nonwoven geotextile-reinforced clay

Figure 8 summarizes the compaction results of nonwoven geotextile-reinforced clay that was compacted in six compaction layers combined with various reinforcement layers under different compaction energies. As the dry unit weight γ_d was evaluated for considering soil only, the

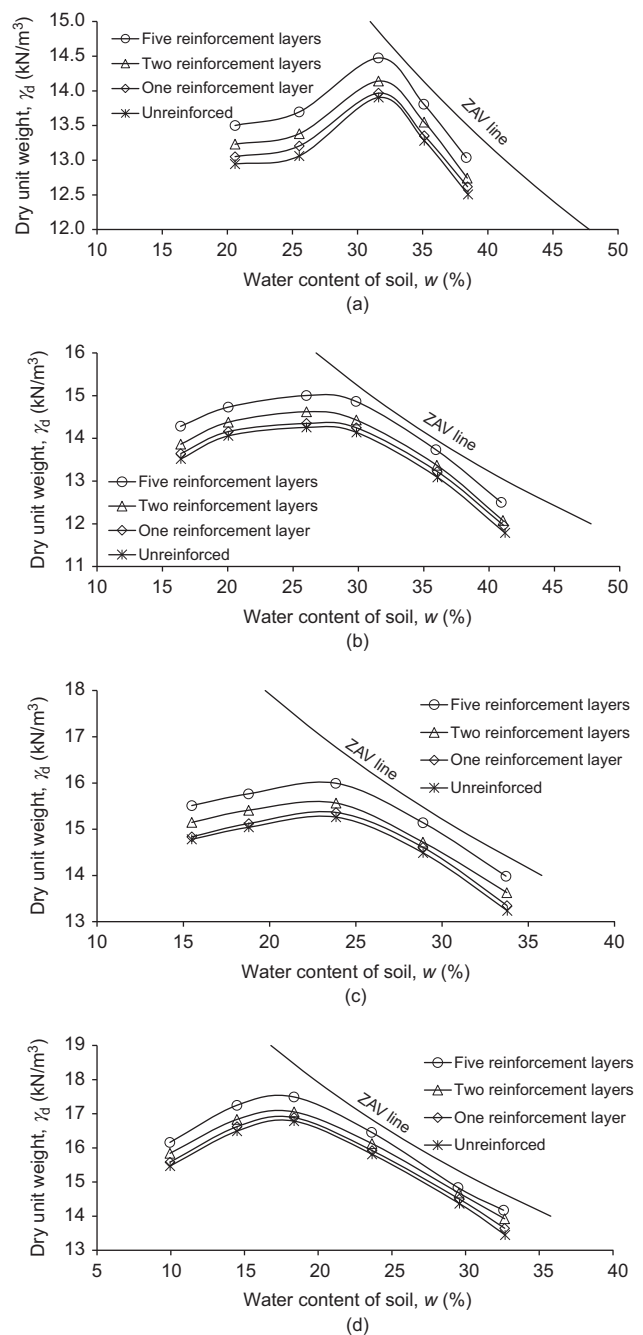


Figure 8. Variation of dry unit weight of unreinforced and reinforced riverbed clay with the water content of soil under different energy energies (a) 600 kJ/m³; (b) 960 kJ/m³; (c) 1920 kJ/m³; and (d) 2700 kJ/m³

test results revealed that, compared with the unreinforced specimen, the density of clay in reinforced specimens increased significantly. The greater the number of reinforcement layers, the higher the increase in the density of the reinforced specimens, especially for reinforced clay specimens with five reinforcement layers. This finding agrees with the results of several studies (Indraratna *et al.* 1991; Keskin *et al.* 2009). This is because the geotextile layers enhanced the dissipation of air and excess pore water pressure during compaction, thereby improving the reduction in porosity of reinforced specimens. The effect of the water dissipation of

reinforcement layers on improving the compaction of reinforced specimens is further evaluated in the next section.

The enhancement of the dry density of reinforced clay was also reduced by the extra confinement generated by the tensile mobilization of reinforcement during compaction. Due to the interface interaction between the reinforcement and the soil, the shear flow of soil is restrained in the lateral direction. As a result, the compaction force compresses the soil more efficiently to expel the void from the soil. As shown in Figure 9, a similar lateral restraint mechanism in geosynthetic-reinforced flexible pavements was proposed in several studies (Holtz *et al.* 1998; Perkins 1999; Zornberg 2011). When vehicle loads are supported, the shear interaction developing between the aggregate and the geosynthetic induces tension in the reinforcement and, in turn, a reduction in the lateral spreading (i.e. increased horizontal stress σ_h and decreased horizontal strain, ϵ_h) of the base aggregate.

A similar reinforcement deformation behavior was observed in the compaction of reinforced clay specimens. The expansion of reinforcement layers in the reinforced specimens indicated the development of tension in the reinforcement layers due to a soil-reinforcement interaction under compaction forces (Figure 10a). As a result, the compacted soil was restrained laterally by the reinforcement layers, and the density of the reinforced soil increased accordingly. Figure 10b shows that geotextile discs not only expanded in plane but also concavely under the dynamic force from compaction. The deformation shapes of the reinforcement layers were also different when the water content of soil and compaction energies were changed. The higher the water content of the soil, the softer it became. As a result, the rammer penetrated the soil more deeply during compaction. Reinforcement layers would be deformed more concavely in specimens with higher water content. Some reinforcement layers broke under the compaction force of the dropping rammer, especially in specimens with a water

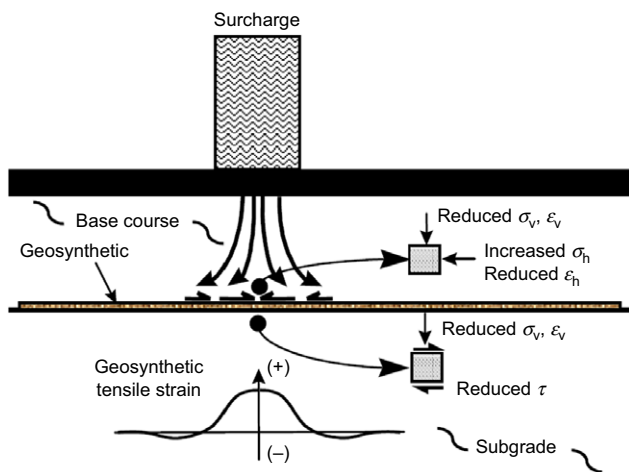


Figure 9. Shear-resisting interface mechanism of reinforcement due to vehicle load (after Perkins 1999)

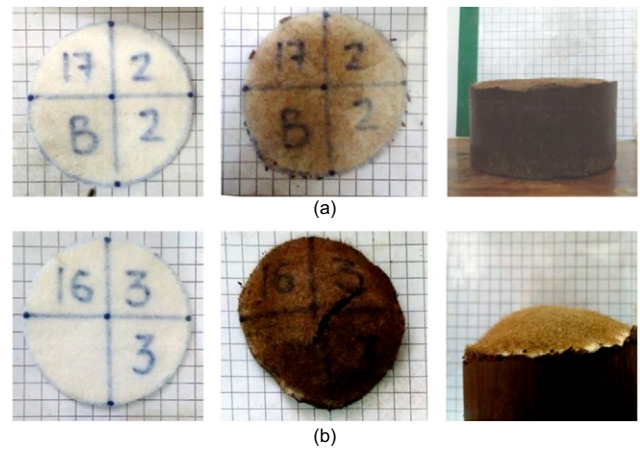


Figure 10. Undeformed (left) and deformed post-test (centre) geotextile disc in specimens reinforced by two layers under 1920 kJ/m³ of compaction energy (a) $w = 20.6\%$ and (b) $w = 38.4\%$; dismantled specimen (right) with geotextile disc

content of over 38% and high compaction energy (Figure 10b).

In Figure 8, it is also observed that the optimum water content w_{opt} changed only marginally between unreinforced and reinforced specimens. Indraratna *et al.* (1991) reported a similar observation when investigating the compaction behavior of soft marine clay reinforced with woven and nonwoven geotextiles. This can be explained as the soil structure remaining unchanged despite the presence of reinforcement inclusions. The geotextile layers only helped to increase the soil density by enhancing air and water pressure dissipation and confinement from mobilizing reinforcement tension. In addition, due to the insignificant difference (i.e. $<0.3\%$) between the water content of unreinforced and reinforced specimens, the presence of geotextile layers also did not significantly influence the w_{opt} value. By contrast, changes in the optimum water content of soil reinforced by various types of fibers have been reported differently in previous studies. Several studies (Ramesh *et al.* 2010; Chaple and Dhattrak 2013; Devdatt *et al.* 2015; Tilak *et al.* 2015) reported the w_{opt} of fiber-reinforced specimens to be slightly higher than that of unreinforced specimens, but some studies reported that the added fiber causes a decrease in the w_{opt} of reinforced fiber soil (Maher and Ho 1994; Nataraj and McManis 1997; Plé and Lê 2012). Changes in w_{opt} of reinforced fiber soil are caused by the different structure of the fiber-soil mixture. Furthermore, the w_{opt} of fiber-reinforced specimens was varied because the dry unit weight of soil reinforced with fiber was evaluated from the entire weight of the soil-fiber mixture without separating the dry weight and volume of reinforcement layers from the reinforced specimens.

Regarding the influence of compaction energy, the dry densities of specimens increased with the applied compaction energy for both unreinforced and reinforced specimens. The w_{opt} value of specimens reduced from 31.6% to 18.4% when the compaction energy was increased from 600 kJ/m³ to 2700 kJ/m³, respectively. Similar findings were reported in numerous studies on the compaction

behavior of clay (Attom 1997; Drew and White 2005; Bera 2014; Sabat and Moharana 2015; Vinod *et al.* 2015; Hussain 2017).

3.3. Compaction effectiveness improvement and compaction energy saving

The compaction improvement of reinforced soil was further analyzed using the maximum dry unit weight, γ_{d-max} . As shown in Figure 11, compared with unreinforced soil, the γ_{d-max} value of reinforced soil was higher and increased with the compaction energy E and number of reinforcement layers. As discussed previously, the density of reinforced soil improved due to water and air dissipation through the reinforcement layers and enhanced confinement from the soil and reinforcement interaction.

The improvement in maximum dry unit weight of compacted soil due to the inclusion was also quantified using the percentage of maximum dry unit weight improvement as

$$\%DD_{re} = \frac{\gamma_{d-max}^{re} - \gamma_{d-max}^{unre}}{\gamma_{d-max}^{unre}} \times 100\% \quad (13)$$

in which γ_{d-max}^{re} and γ_{d-max}^{unre} are the maximum dry unit weight of reinforced and unreinforced soil specimens (compacted under the same compaction energy), respectively.

The results revealed that the improvement in maximum dry unit weight of reinforced clay decreased with an increase in reinforcement spacing, h (Figure 12) which was defined as

$$h = \frac{H}{n_r + 1} \quad (14)$$

where n_r = number of reinforcement layers in the reinforced specimen.

Compared to the influence of h , the influence of compaction energy on $\%DD_{re}$ is minor. The improved density of reinforced soil increased when the reinforcement spacing was reduced. For $h = 19.43$ mm, the improvement density of reinforced soil reached the maximum value of 4.3–5.3% regardless of the compaction

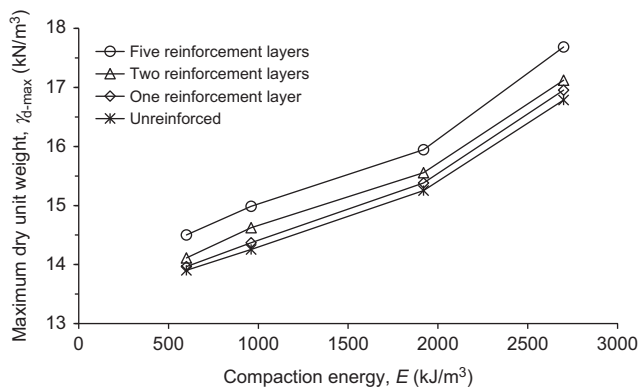


Figure 11. Variation of maximum dry unit weight of unreinforced and reinforced clay under different compaction energies

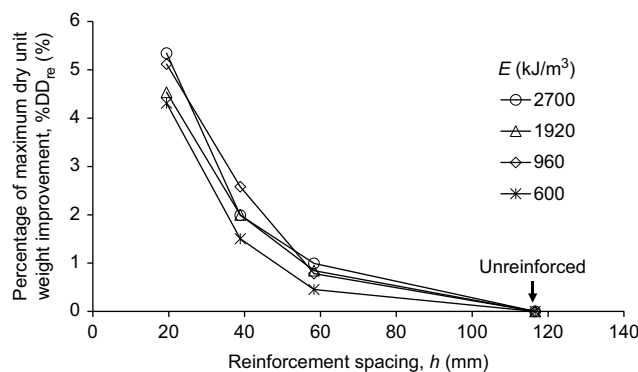


Figure 12. Variation of percentage of dry unit weight improvement with reinforcement spacing. The unreinforced specimens were equivalent to a reinforcement spacing of 116.6 mm

energy level. The variation of $\%DD_{re}$ was small (less than 1%) when the compaction energy was changed from 600 to 2700 kJ/m^3 .

The test result showed that for the same compaction energy, the maximum density of reinforced clay was higher than that of unreinforced soil. In other words, to reach the same maximum dry unit weight of compacted soil, the compaction energy applied to unreinforced soil specimens was higher than that applied to reinforced soil specimens. In order to evaluate the level of reduction of compaction due to reinforcement, the value of compaction energy of unreinforced and reinforced soil to achieve the same maximum dry unit weight was calculated using the data shown in Figure 11. At a maximum dry unit weight of unreinforced specimens, γ_{d-max}^{unre} , the value of $E_{\gamma_{d-max}^{unre}}^{unre}$ were determined as 600, 960, 1920 or 2700 kJ/m^3 . The values of $E_{\gamma_{d-max}^{re}}^{re}$ were evaluated by interpolating the compaction energy of reinforced specimens with the value of γ_{d-max}^{unre} . Besides, for a maximum dry unit weight of reinforced specimens, γ_{d-max}^{re} equivalent to a compaction energy level (i.e. $E_{\gamma_{d-max}^{re}}^{re}$), the value of $E_{\gamma_{d-max}^{re}}^{unre}$ was interpolated using the value of γ_{d-max}^{re} . Since the compaction energy in the test was varied from 600 to 2700 kJ/m^3 , the evaluated compaction energy should also be limited in that range of values. The reduction in compaction energy due to reinforcement was then evaluated using the percentage of compaction energy saving $\%E_s$:

$$\%E_s = \frac{E_{\gamma_{d-max}^{unre}}^{unre} - E_{\gamma_{d-max}^{re}}^{re}}{E_{\gamma_{d-max}^{re}}^{unre}} \quad (15)$$

As shown in Figure 13, the larger the number of reinforcement layers, the higher the compaction energy saving. The level of compaction energy saving generally reduced when the compaction energy was increased from 600 kJ/m^3 (i.e. standard compaction) to 2700 kJ/m^3 (i.e. modified compaction). At standard compaction energy, the compaction energy could be reduced by up to 10.4% and 27.0% when compacting clay with one and two reinforcement layers, respectively. In particular, when using five reinforcement layers during compaction at 600 kJ/m^3 , almost half of the compaction energy (i.e. 49.9%) can be saved. At the modified compaction energy $E = 2700 \text{ kJ/m}^3$, the compaction energy saving

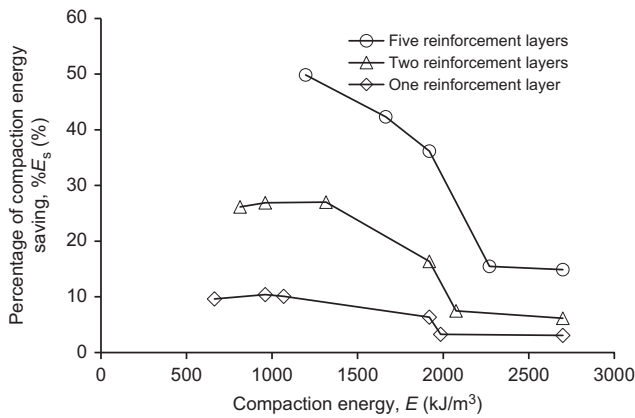


Figure 13. Effect of number of reinforcement layers on the percent of compaction energy saving

reduced to 3.1%, 6.2%, and 14.9% when one, two, and five reinforcement layers were used to compact the clay specimens, respectively.

4. WATER ABSORPTION IN THE REINFORCEMENT LAYERS

The influence of reinforcement on improving the effectiveness of soil compaction was further assessed by investigating the degree of saturation of soil specimens and water absorption in the reinforcement layers.

4.1. Degree of saturation of unreinforced and reinforced specimens

As discussed previously, the optimum degree of saturation of compacted specimens is an important parameter for ensuring the maximum saturated stiffness/strength of a given soil type. The degree of saturation of specimens was evaluated as

$$S_r = \frac{G_s w}{e} \quad (16)$$

in which G_s is the specific gravity of clay ($=2.75$); w and e are the water content and void ratio of soil in both unreinforced and reinforced specimens, respectively.

The variation of the degree of saturation of unreinforced and reinforced specimens, S_r , with the value of $w - w_{opt}$ is shown in Figures 14–17. In general, S_r increases with an increase in the water content of soil, w . In particular, S_r is less than 70% when w is smaller than w_{opt} by 5%. On the wet side of the optimum water content, the compacted specimens were relatively saturated ($S_r > 90\%$) when w was 5% higher than w_{opt} .

The degree of saturation S_r of reinforced specimens increases with the number of reinforcement layers. It can be explained as the improvement of the density of the reinforced specimens (i.e. lower void ratio e) over the unreinforced specimens, which reduced the void volume (including water and air) in the soil specimens. The reduction of air voids apparently dominated the total void reduction because the water content of soil does not

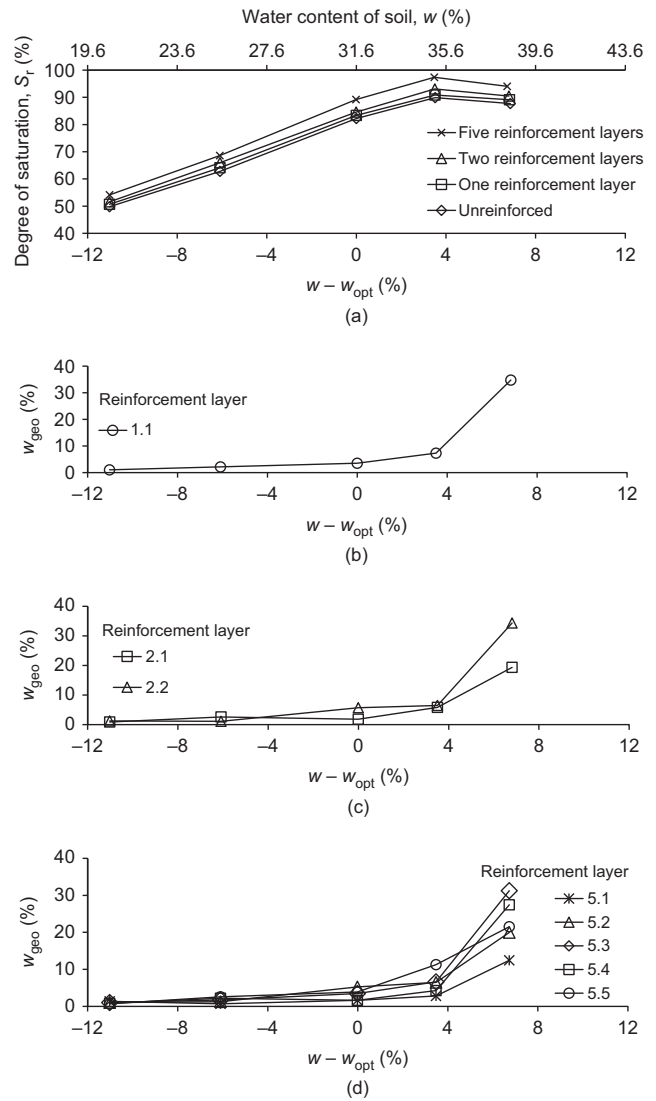


Figure 14. Variation of (a) degree of saturation and water content of geotextile layers in specimens reinforced with (b) single reinforcement layer; (c) two reinforcement layers; and (d) five reinforcement layers under 600 kJ/m³ of compaction energy

change significantly over the unreinforced and reinforced specimens, as discussed previously.

In addition, the degree of saturation S_r slightly decreases when $w - w_{opt}$ is over 5–10%. Because the clay was too wet and soft, it was difficult to further expel air voids under compaction forces.

Tatsuoka and Correia (2016) defined the optimum degree of saturation of compacted specimens $S_{r(opt)}$ as S_r at which the maximum dry unit weight is obtained. In other words, $S_{r(opt)}$ is determined from the specimen at its optimum water content w_{opt} . Figure 18 shows the $S_{r(opt)}$ value of unreinforced and reinforced specimens with different levels of compaction energy. The result shows that $S_{r(opt)}$ varies marginally with the compaction energy level E . The average $S_{r(opt)}$ value of unreinforced soil is 81.3%, which is close to the average $S_{r(opt)}$ value of 82% proposed by Tatsuoka and Correia (2016). The average $S_{r(opt)}$ value increases with the number of reinforcement layers, and it is 82.7%, 85.0%, and 90.6% for specimens

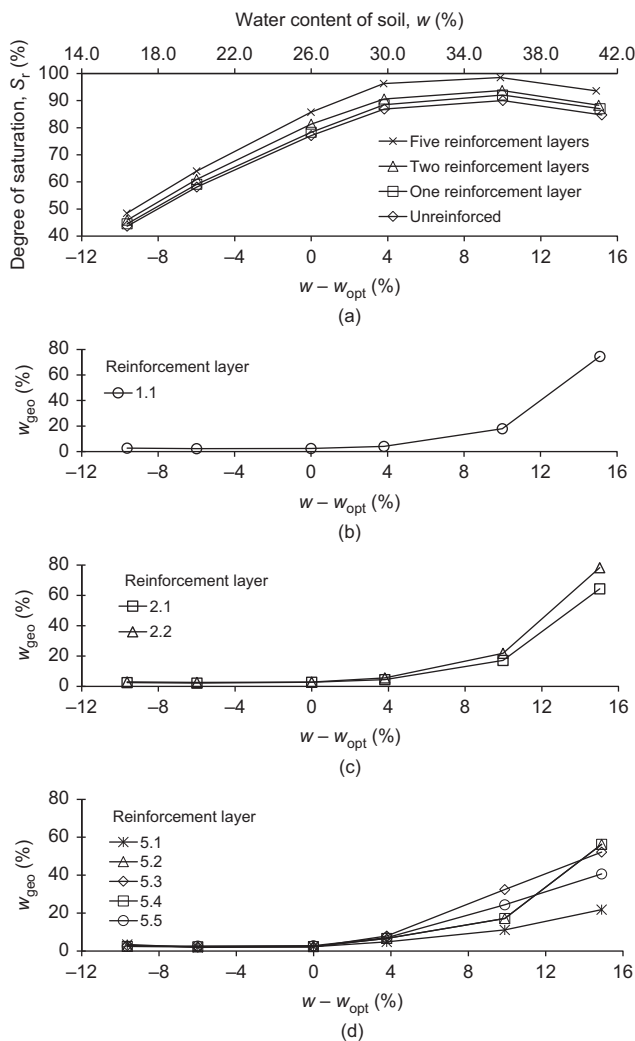


Figure 15. Variation of (a) degree of saturation and water content of geotextile layers in specimens reinforced with (b) single reinforcement layer; (c) two reinforcement layers; and (d) five reinforcement layers under 1200 kJ/m³ of compaction energy

reinforced with one, two, and five layers, respectively (Table 4).

4.2. Water content of reinforcement layers

The water contents of geotextile layers w_{geo} in specimens reinforced with one, two, and five reinforcement layers are shown in Figures 14–17. In general, the water content of the geotextile layer increases with the water content of soil specimens.

Two water drainage mechanisms were used to explain the test results observed: (1) direct contact between reinforcement and wet soil and (2) dissipation of water pressure into the permeable reinforcement under dynamic compaction forces. Figures 14–17 show that when the water content of the soil sample is less than its OMC, the water content of geotextile layers w_{geo} is small (less than 4%) and increases slightly even with 10% increment of the water content of soil. The water content of reinforcement layers also did not increase when the compaction energy was increased. It seems that at this water content range, the amount of water was not sufficient to fill voids fully in

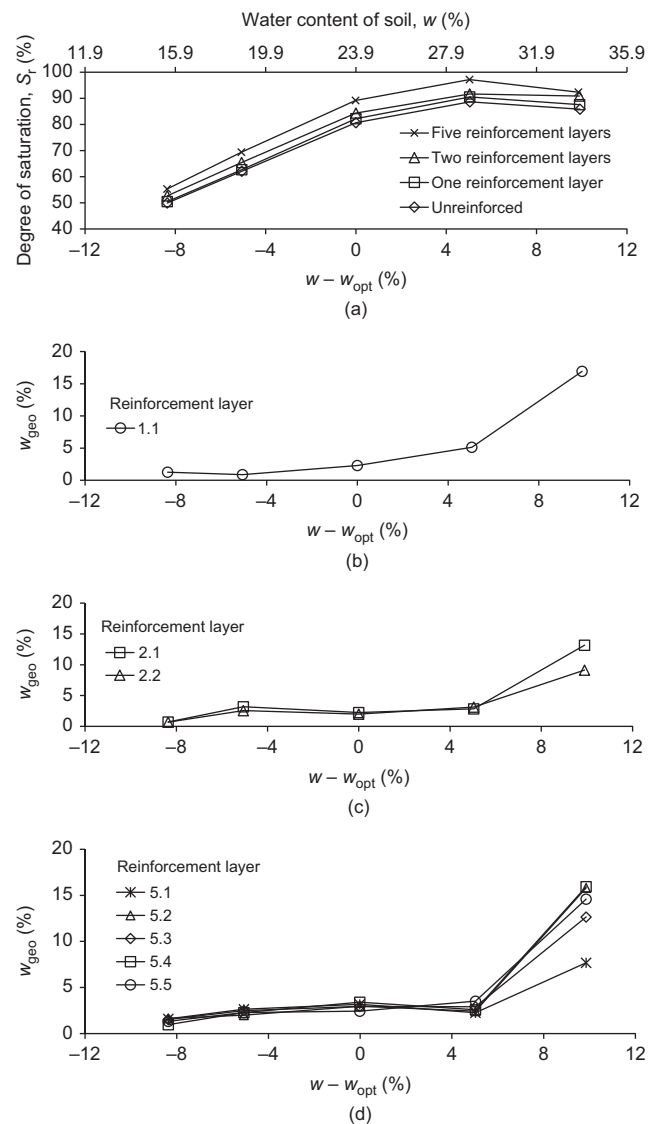


Figure 16. Variation of (a) degree of saturation and water content of geotextile layers in specimens reinforced with (b) single reinforcement layer; (c) two reinforcement layers; and (d) five reinforcement layers under 1920 kJ/m³ of compaction energy

soil specimens (i.e. less than a 90% degree of saturation of soil specimens). As a result, the excess pore water pressure did not increase and dissipated into the geotextile discs during compaction. Therefore, only a small amount of water was observed in the geotextile layers due to direct contact between the reinforcement and wet soil.

By contrast, in this study, when the water content was higher than w_{opt} by 5–10%, the water content of the geotextile layer increased significantly with an increase in the water content of soil and compaction energy level. The water content of the geotextile layer increased sharply when soil specimens had a degree of saturation of over 90% (i.e. almost fully saturated). Under dynamic compaction forces, the pores between the aggregate were reduced and became small, soil pores were filled with water, and pore water pressure increased. Earlier studies have already reported and approved an increase in pore water pressure when compacting saturated and partially saturated soil.

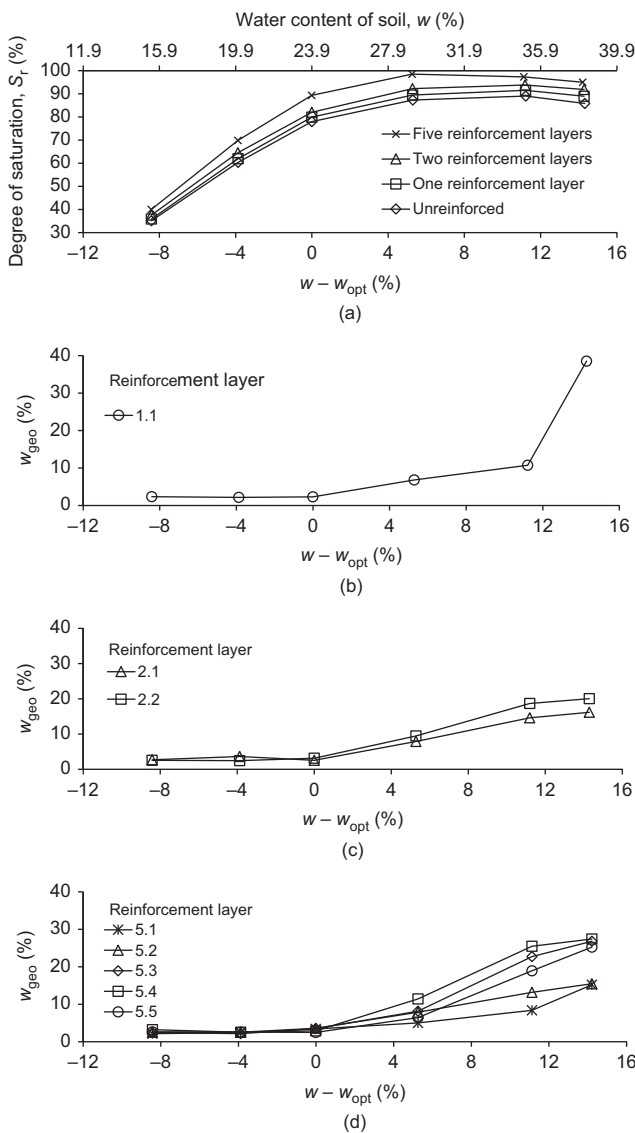


Figure 17. Variation of (a) degree of saturation and water content of geotextile layers in specimens reinforced with (b) single reinforcement layer; (c) two reinforcement layers; and (d) five reinforcement layers under 2700 kJ/m³ of compaction energy

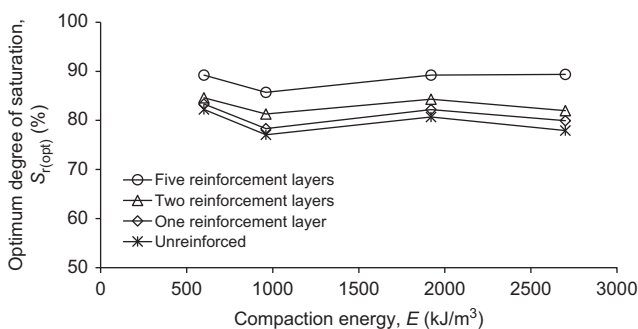


Figure 18. Variation of optimum degree of saturation of unreinforced and reinforced compacted specimens under different compaction energy

Other studies have reported similar observations. Table 5 shows changes in the degree of saturation of partially saturated clay under isotropic compression with

air drainage, as evaluated from test data by Lins and Sandroni (1994). This reveals that S_r increased significantly after applying isotropic compression pressure on unsaturated clay specimens. Furthermore, excess pore water pressure occurred when the degree of saturation of soil specimens was over $\sim 90\%$. Li *et al.* (2011) noted excess pore water pressure when clay was compacted below ground water level (i.e. saturated soil). Under ramming strike compaction, the excess pore water pressure increased with an increase in the compaction number and decrease in strata depth.

In summary, when the water content was lower than the optimum moisture content, less than 4% of the water content of the reinforcement layers in reinforced soil specimens was observed due to water absorption from the direct contact between wet soil and dry reinforcement layers. When the water content of soil was higher than the w_{opt} by 5–10%, which was equivalent to a degree of saturation of over 90%, excess pore water pressure occurred during compaction. As a result, the water content of reinforcement layers increased significantly, indicating that the permeable reinforcement dissipated excess pore water in compacted clay.

4.3. Improvement of soil void ratio by reinforcement

Apart from dry unit weight, void ratio is also used to evaluate the compaction effectiveness of soil, as suggested by Walker and Chong (1986). The void ratio of unreinforced and reinforced specimens was evaluated based on their dry unit weight.

$$e = \frac{G_s \gamma_w}{\gamma_d} - 1 \tag{17}$$

The effect of reinforcement on reducing the void ratio of reinforced soil was evaluated using the void ratio reduction percentage $\% \Delta e$:

$$\% \Delta e = \frac{e_{unre} - e_{re}}{e_{unre}} \times 100\% \tag{18}$$

where e_{unre} and e_{re} are the void ratio of unreinforced and reinforced specimens compacted at the same initial water content, respectively.

Figure 19 shows the improvement of the void ratio of reinforced soil at the optimum water content. In general, when increasing the compaction energy from 600 to 2700 kJ/m³, the void ratio reduction percentage increased. The greater the number of reinforcement layers, the higher the void ratio improvement and the denser the compacted soil. When reinforced by a single layer, only 0.9–2.5% of void ratio reduction of reinforced clay was observed. For specimens reinforced with two and five reinforcement layers, void ratio reductions showed a significant improvement of 3.0–5.0% and 8.3–13.1%, respectively.

Furthermore, to quantify the effect of water absorption of reinforcement layers on the void ratio improvement of compacted soil, air and water voids were evaluated separately within the total voids in compacted soil. The air void ratio e_a was defined as the ratio of the volume of air to the volume of solid soil. The water void ratio e_w was

Table 4. Values of optimum degree of saturation of unreinforced and reinforced specimens

| Specimens | Compaction energy level, (kJ/m ³) | | | | Average $S_{r(opt)}$, (%) |
|-----------------------|---|------|------|------|----------------------------|
| | 600 | 960 | 1920 | 2700 | |
| Unreinforced | 87.3 | 77.1 | 81.7 | 79.2 | 81.3 |
| Reinforced – 1 layer | 88.1 | 78.3 | 83.2 | 81.2 | 82.7 |
| Reinforced – 2 layers | 90.0 | 81.3 | 85.4 | 83.3 | 85.0 |
| Reinforced – 5 layers | 95.2 | 85.7 | 90.4 | 91.0 | 90.6 |

Table 5. Changes of void ratio and degree of saturation of partial saturated clayey soil analyzed using data from Lins and Sandroni (1994)

| Water content, (%) | Test case | At the beginning of test | | When excess pore water pressure occurs | |
|--------------------|-----------------|--------------------------|-------------|--|--------------------------|
| | | Void ratio, e | S_r , (%) | Void ratio, e | S_r , (%) ^a |
| 30.2 | $w_{opt} + 2.4$ | 0.97 | 83.0 | 0.90 | 89.1 |
| 27.5 | $w_{opt} - 0.3$ | 0.89 | 84.7 | 0.83 | 90.9 |
| 25.4 | $w_{opt} - 2.4$ | 0.93 | 75.0 | 0.80 | 86.8 |
| 24.3 | $w_{opt} - 3.5$ | 0.94 | 71.0 | 0.75 | 89.6 |
| 23.3 | $w_{opt} - 4.5$ | 0.98 | 65.2 | 0.72 | 89.0 |

^aEstimated values from Lins and Sandroni 1994.

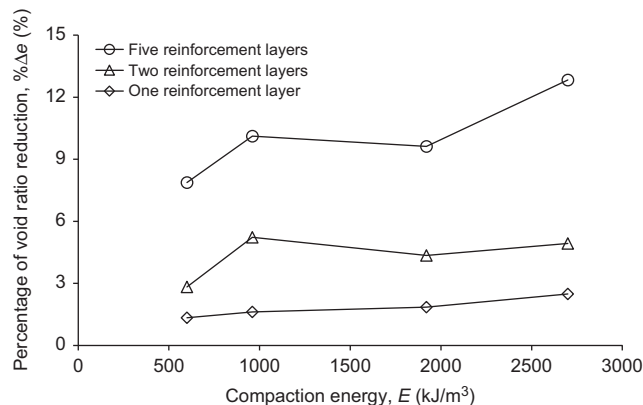


Figure 19. Percentage of void ratio reduction of reinforced soil compacted at the optimum water content OMC under different compaction energy, E

defined as the ratio of the volume of water to the volume of soil particles. The water void ratio of both unreinforced and reinforced specimens was evaluated from the water content w .

$$e_w = wG_s \tag{19}$$

where G_s is the specific gravity of the soil.

Although being compacted at the same water content, the water content of reinforced soil was lower than that of unreinforced soil due to water absorption by the reinforcement layers. As a result, the reduction in water void ratio due to permeable reinforcement can be calculated based on the difference between the water content of reinforced and unreinforced soil after compaction.

$$\Delta e^w = \frac{w_{geo} W_{d-geo}}{W_{d-soil}} G_s \tag{20}$$

The water drainage effect of reinforcement during compaction was assessed using the void ratio improvement percentage from water absorption $\% \Delta e^w$, which was defined as the ratio of water void ratio reduction to void ratio reduction between reinforced soil and unreinforced soil under the same water content and compaction energy.

$$\% \Delta e^w = \frac{\Delta e^w}{e_{unre} - e_{re}} 100\% \tag{21}$$

Figure 20 shows that the void ratio improvement percentage from water absorption $\% \Delta e^w$ increased with the water content of reinforced soil. Equations 21 and 22 indicate that the value of Δe^w strongly correlated with the water absorption in reinforcement layers during compaction. Therefore, the variation of Δe^w with the water content of reinforced soil in Figure 20 was similar to that of w_{geo} shown in Figures 14–17. With the increment in the water content of soil, the water content of the reinforcement layers also increased, which induced the higher Δe^w . Besides, a water content of soil higher than w_{opt} by 5–10% is also the threshold value at which the void ratio improvement percentage from water absorption increased dramatically due to the dissipation of excess pore water pressure by the reinforcement layers (Figure 20).

In general, for the same difference between the water content of reinforced soil and the w_{opt} value, the higher the compaction energy, the lower the void ratio improvement from the absorption of water by reinforcement layers. Under standard compaction energy $E = 600 \text{ kJ/m}^3$, $\% \Delta e^w$ could be 4.5–5.6% when $w - w_{opt}$ was ~6.7%. To reach this $\% \Delta e^w$ value, $w - w_{opt}$ must be approximately 12–13% for reinforced soil under compaction energy $E = 960 \text{ kJ/m}^3$. For $E = 1920$ and 2700 kJ/m^3 , to increase $\% \Delta e^w$ by 2–3%, the difference between w and w_{opt} should be larger than 10%.

The number of reinforcement layers in soil specimens did not seem to influence $\% \Delta e^w$. Under a given compaction energy value, the variation of $\% \Delta e^w$ of clay reinforced by different numbers of reinforcement layers was less than 2% and increased with an increase in the water content of reinforced soil specimens (Figure 20).

Finally, as shown in Figure 21, for the same water content of reinforced soil, an increase in compaction energy led to an increase in $\% \Delta e^w$. This is because more water content was absorbed into the reinforcement layer due to the higher dynamic compaction force.

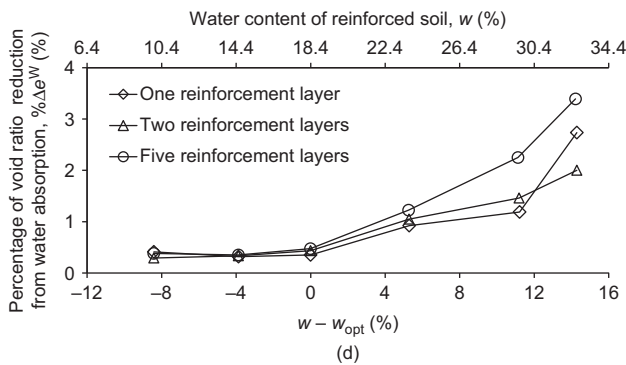
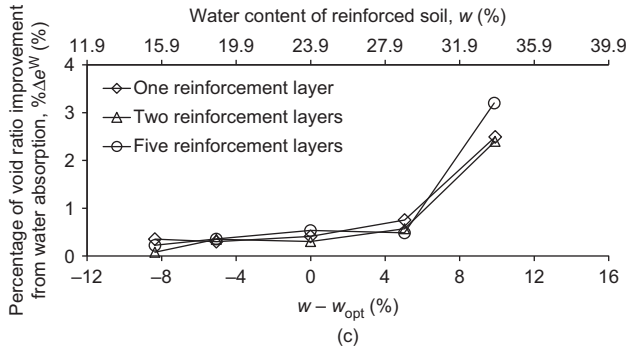
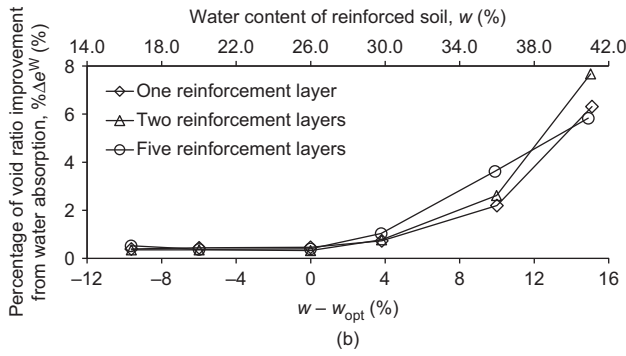
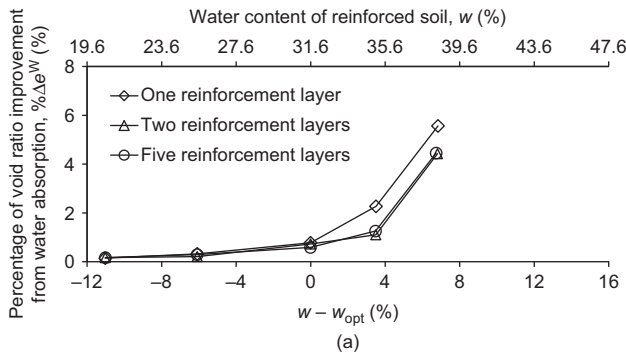


Figure 20. Variation of percentage of water void ratio reduction with water content of soil in reinforced specimens using (a) standard compaction energy, $E = 600 \text{ kJ/m}^3$, and modified compaction energy (b) $E = 960 \text{ kJ/m}^3$; (c) $E = 1920 \text{ kJ/m}^3$; and (d) $E = 2700 \text{ kJ/m}^3$

The difference markedly increased for reinforced soil with higher water content.

5. CONCLUSIONS

In this study, a series of compaction tests were conducted with clay specimens reinforced with nonwoven geotextiles.

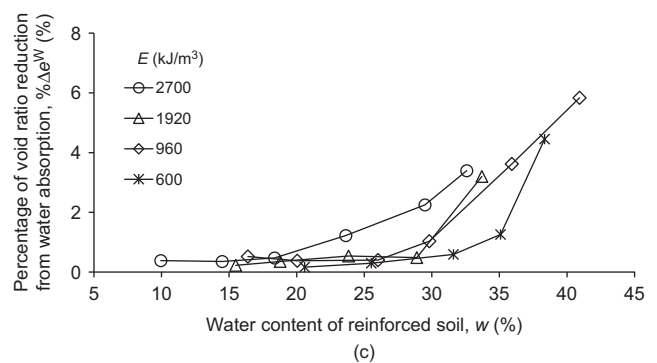
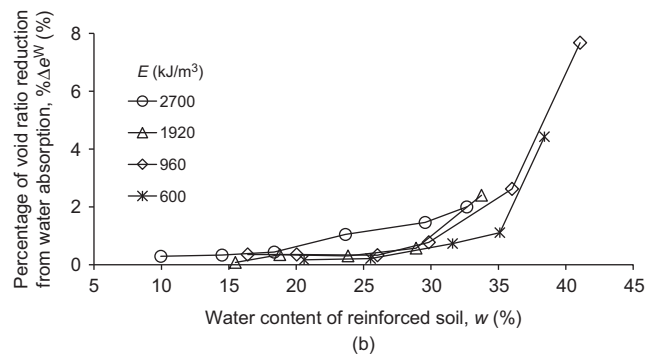
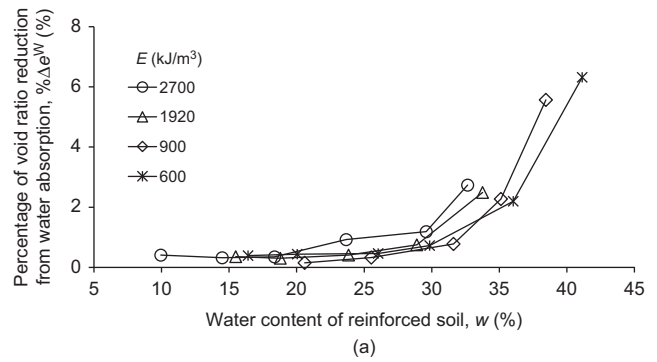


Figure 21. Variation of percentage of water void ratio reduction with water content of soil specimens reinforced by (a) single reinforcement layer; (b) two reinforcement layers; and (c) five reinforcement layers

This study aimed to assess the effect of permeable reinforcement on the improvement of compaction behavior of reinforced clay. The following conclusions are drawn from this study.

- (1) For the unreinforced soil under the same compaction energy, the lift thickness of each compaction layer changed the optimum water content w_{opt} only slightly. The smaller the spacing among compaction layers, the higher the dry unit weight of specimens. At the optimum water content, the dry unit weight improvement was highest, and it decreased with an increase in the $w - w_{opt}$ value.
- (2) The compaction behavior of reinforced specimens was assessed from the soil alone between reinforcement layers. The results revealed that the optimum water content of reinforced clay w_{opt} changed marginally compared with that of

unreinforced specimens due to the small difference (i.e. <0.3%) between the water content of unreinforced and reinforced specimens. For both unreinforced and reinforced specimens, the increase in compaction energy induced higher dry densities and lower ω_{opt} of specimens.

- (3) Under dynamic forces during compaction, the reinforcement discs not only deformed significantly in plane but also concavely in the cross-plane direction, indicating the mobilization of tensile force in the reinforcement layers. The density of reinforced soil was enhanced, which was attributed to the restrained expansion of soil between reinforcement layers under compaction forces. Compared with that of unreinforced specimens, reinforcement improved the maximum dry unit weight by up to 4.5–5.3% when soil specimens were reinforced by five reinforcement layers.
- (4) The use of nonwoven geotextile layers during compaction of clay could significantly reduce compaction energy. The greater the number of reinforcement layers, the greater the compaction energy saving. The compaction energy saving percentage reached up to 50% when clay was compacted with five reinforcement layers under standard compaction energy. It was reduced to 14.9% when the compaction energy was increased to 2700 kJ/m³.
- (5) The degree of saturation of reinforced specimens was higher than that of unreinforced soil for the same water content and compaction energy level. The average value of optimum degree of saturation $S_{r(opt)}$ of unreinforced clay was 81.3%, and it varied marginally with an increase in the compaction energy level.
- (6) The geotextile layers were observed to absorb water during the compaction of reinforced clay. At $w < w_{opt}$, the degree of saturation of soil specimens was less than 90%, and only a small amount of water was absorbed in the geotextile layers (i.e. <4% of water content in geotextile layers) due to direct contact between the wet soil and the dry reinforcement layers. When the $w > w_{opt}$ by 5–10%, and the $S_r \geq 90\%$, the water content of the reinforcement layer increased sharply, resulting in excess pore water pressure in the soil mass and partial dissipation through the permeable nonwoven geotextile layers.
- (7) The larger the number of reinforcement layers, the higher the void ratio improvement percentage. The inclusion reduced both the air void ratio (through the air permeability of the reinforcement layers) and the water void ratio (as the water was absorbed into the permeable reinforcement layers).

The presented findings are limited to the laboratory test scale, which is different from the field condition. For instance, the reinforcement spacing of specimens in the laboratory compaction tests is smaller than that in the

field. The field condition induces a higher reinforcing effect on the compaction behavior of reinforced soil than in the laboratory. In addition, due to the different boundary conditions, the reinforcement in the field appears to be more effective in restraining the lateral expansion of soil than in the compaction mold in the laboratory. Finally, the compaction energy, soil properties, and applied water content in the field are likely less uniform and homogeneous compared to the laboratory condition.

ACKNOWLEDGEMENT

This research is funded by Vietnam National Foundation for Science and Technology Development (NAFOSTED) under grant number 107.01-2016.31. The equipment for the laboratory testing program is supported by Ministry of Education and Training (MOET) under grant number B2017.SP.K.02.

NOTATION

Basic SI units are given in parentheses.

| | |
|--|--|
| $\%DD_L$ | percentage of dry unit weight difference (dimensionless) |
| $\%DD_{re}$ | percentage of maximum dry unit weight improvement (dimensionless) |
| d | diameter of reinforcement layer (m) |
| E | compaction energy (J/m ³) |
| $\%E_s$ | percentage of compaction energy saving (dimensionless) |
| $E_{\gamma d-max}^{unre}, E_{\gamma d-max}^{re}$ | compaction energy applied to unreinforced soil and reinforced soil, respectively (J/m ³) |
| e | void ratio of soil specimens (dimensionless) |
| e_a, e_w | air void ratio and water void ratio, respectively (dimensionless) |
| e_{unre}, e_{re} | void ratio of unreinforced and reinforced specimens, respectively (dimensionless) |
| G_s | specific gravity (dimensionless) |
| H | total height of compacted specimen (m) |
| h | reinforcement spacing (m) |
| h_{re} | depth of geotextile layer in compacted specimens (m) |
| i | ordinal number (dimensionless) |
| k | cross-plane permeability geotextile (m/sec) |
| k_{sat} | saturated hydraulic conductivity of clay (m/sec) |
| LL, PL, PI | liquid limit, plastic limit, and plasticity index, respectively (dimensionless) |
| l | lift thickness (m) |

| | |
|--|--|
| n_c, n_r | number of compacted layers and number of reinforcement layers in specimens, respectively (dimensionless) |
| OMC | optimum moisture content (dimensionless) |
| S_r | degree of saturation of soil (dimensionless) |
| $(S_r)_{opt}$ | optimum degree of saturation of soil (dimensionless) |
| t_i, t_{min}, t_{max} | actual, minimum, and maximum thickness of a geotextile layer, respectively (m) |
| V | mold volume (m^3) |
| V_{geo} | total volume of all reinforcement layers (m^3) |
| W_{d-geo} | dry weight of geotextile layers (N) |
| W_{d-soil} | total weight of dry soil (N) |
| W, W_{re} | moisture weight of unreinforced specimens and reinforced specimens, respectively (N) |
| $W_{w,tested_geo}$ | weight of wet and dry geotextile layers, respectively (N) |
| $W_{d,tested_geo}$ | weight of dry geotextile layers, respectively (N) |
| w | water content of soil specimens (dimensionless) |
| w_{geo} | water content of geotextile layers (dimensionless) |
| w_{opt} | optimum moisture content (dimensionless) |
| γ, γ_d | bulk and dry unit weight of soil, respectively (N/m^3) |
| γ_{d-max} | maximum dry unit weight of compacted soil (N/m^3) |
| $\gamma_{d-max}^{re}, \gamma_{d-max}^{unre}$ | maximum dry unit weight of reinforced soil and unreinforced soil, respectively (N/m^3) |
| $\gamma_{d-nlayers}$ | dry unit weight of soil compacted by n_c |
| $\gamma_{d-2layers}$ | and two compaction layers, respectively (N/m^3) |
| $\gamma_{d-unre}, \gamma_{d-re}$ | dry unit weight of unreinforced and reinforced specimens, respectively (N/m^3) |
| γ_w | unit weight of water (N/m^3) |
| Δe^0 | void ratio reduction percentage (dimensionless) |
| Δe^w | reduction in water void ratio (dimensionless) |
| $\% \Delta e^w$ | percentage of void ratio improvement from water absorption (dimensionless) |
| Δw | water content reduction (dimensionless) |
| ε_h | horizontal strain (dimensionless) |
| σ_h | horizontal stress (Pa) |
| σ_{ti} | standard deviation of the geotextile thickness (dimensionless) |
| σ_v | overburden pressure (Pa) |
| $\sigma_{\gamma d-re}$ | standard deviation of dry unit weight of reinforced soil specimen (N/m^3) |
| τ | the shear stress in the subgrade soil (Nm^2) |
| ψ | permittivity of geotextile (sec^{-1}) |

ABBREVIATIONS

ZAV zero air voids

REFERENCES

- AASHTO (2002). *Standard Specifications for Highway Bridges*, 17th edn., AASHTO, Washington, DC, USA.
- ASTM D 422 *Standard Test Method for Particle-Size Analysis of Soils*. ASTM International, West Conshohocken, PA, USA.
- ASTM D 698 *Standard Test Methods for Laboratory Compaction Characteristics of Soil Using Standard Effort (12 400 ft-lbf/ft³, 600 kN-mlm³)*, ASTM International, West Conshohocken, PA, USA.
- ASTM D 1557 *Standard Test Methods for Laboratory Compaction Characteristics of Soil Using Modified Effort (56 000 ft-lbf/ft³ 2700 kN-mlm³)*. ASTM International, West Conshohocken, PA, USA.
- ASTM D 2216 *Standard Test Methods for Laboratory Determination of Water (Moisture) Content of Soil and Rock by Mass*. ASTM International, West Conshohocken, PA, USA.
- ASTM D 4491 *Standard Test Methods for Water Permeability of Geotextiles by Permittivity*. ASTM International, West Conshohocken, PA, USA.
- ASTM D 4595 *Standard Test Method for Tensile Properties of Geotextiles by the Wide-Width Strip Method*. ASTM International, West Conshohocken, PA, USA.
- Attom, M. F. (1997). The effect of compactive energy level on some soil properties. *Applied Clay Science*, **12**, No. 1–2, 61–72.
- Bera, A. K. (2014). Compaction characteristics of fine grained soil and rice husk ash mixture. *International Journal of Geotechnical Engineering*, **8**, No. 2, 121–129.
- Berg, R., Christopher, B. R. & Samtani, N. (2009). *Design of Mechanically Stabilized Earth Walls and Reinforced Soil Slopes*, Rep. No. FHWA-NHI-10-024. National Highway Institute, Federal Highway Administration, Washington, DC, USA.
- Blotz, R. L., Craig, H. B. & Boutwell, P. (1998). Estimating optimum water content and maximum dry unit weight for compacted clay. *Journal of Geotechnical and Geoenvironmental Engineering, ASCE*, **124**, No. 9, 907–912.
- Chaple, P. M. & Dhattrak, A. I. (2013). Performance of coir fiber reinforced clayey soil. *The International Journal of Engineering and Science (IJES)*, **2**, No. 4, 54–64.
- Chegenizadeh, A. & Nikraz, H. (2011). Investigation on compaction characteristics of reinforced soil. *Advanced Materials Research*, **261–263**, 964–968.
- D'Appolonia, D. J., Whitman, R. V. & D'Appolonia, E. D. (1969). Sand compaction with vibratory compaction equipment. *Journal of the Soil Mechanics and Foundations Division*, **95**, No. 1, 263–284.
- Devdatt, S., Shikha, R., Saxena, A. K. & Jha, A. K. (2015). Soil stabilization using coconut coir fibre. *International Journal for Research in Applied Science & Engineering Technology*, **3**, No. 9, 305–309.
- Drew, I. & White, D. J. (2005). Influence of compaction energy on soil engineering properties. *Proceedings of the 2005 Mid-Continent Transportation Research Symposium*, Ames, IA, USA, Center for Transportation Research and Education, Ames, IA, USA, pp. 215–216.
- Elias, V., Christopher, B. R. & Berg, R. (2001). *Mechanically Stabilized Earth Walls and Reinforced Soil Slopes Design and Construction Guidelines*, Rep. No. FHWA-NHI-00-043. National Highway Institute, Federal Highway Administration, Washington, DC, USA.
- Fourie, A. B. & Fabian, K. J. (1987). Laboratory determination of clay geotextile interaction. *Geotextiles and Geomembranes*, **6**, No. 4, 275–294.
- Gupta, S. C., Sharma, P. P. & DeFranchi, S. A. (1989). Compaction effects on soil structure. *Advances in Agronomy*, **42**, 311–338.
- Gurtug, Y. & Sridharan, A. (2004). Compaction behavior and prediction of its characteristics of fine grained soils with particular

- reference to compaction energy. *Soil and Foundation*, **44**, No. 5, 27–36.
- Holtz, R. D., Christopher, B. R. & Berg, R. R. (1998). *Geosynthetic Design and Construction Guidelines*, FHWA-HI-98-038. Federal Highway Administration, Washington, DC, USA.
- Holtz, R. D., Kovacs, W. D. & Sheahan, T. C. (2010). *An Introduction to Geotechnical Engineering*, Prentice Hall, Englewood Cliffs, NJ, USA.
- Hussain, S. (2017). Effect of compaction energy on engineering properties of expansive soil. *Civil Engineering Journal*, **3**, No. 8, 610–616.
- Indraratna, B., Satkunaseelan, K. S. & Rasul, M. G. (1991). Laboratory properties of a soft marine clay reinforced with woven and nonwoven geotextiles. *Geotechnical Testing Journal, GTJODJ*, **14**, No. 3, 288–295.
- Iryo, T. & Rowe, R. K. (2005). Infiltration into an embankment reinforced by nonwoven geotextiles. *Canadian Geotechnical Journal*, **42**, No. 4, 1145–1159.
- ISO (International Organization for Standardization) (2016). ISO 9863-1:2016(E). Geosynthetics – Determination of thickness at specified pressures – Part 1: Single layers. ISO, Switzerland
- Jiang, Y., Han, J., Parsons, R. L. & Brennan, J. J. (2016). Field instrumentation and evaluation of modular-block MSE walls with secondary geogrid layers. *Journal of Geotechnical and Geoenvironmental Engineering, ASCE*, **142**, No. 12, 05016002.
- Keskin, S. N., Cimen, O., Goksan, T. S., Uzundurukan, S. & Karpuzcu, M. (2009). Effect of geotextiles on the compaction properties of soils. *2nd International Conference on New Developments in Soil Mechanics and Geotechnical Engineering*, Near East University, Nicosia, North Cyprus, pp. 420–424.
- Lambe, T. W. & Whitman, R. V. (1969). *Soil Mechanics*. John Wiley & Sons, New York, NY, USA.
- Leshchinsky, D. (2000). *Alleviating Connection Load*, Geotechnical Fabrics Report, Industrial Fabrics Association International, St Paul, MN, USA.
- Li, X. J., Yao, K. & Zhu, S. C. (2011). Study on the changing rule of excess pore water pressure during dynamic compaction. *Applied Mechanics and Materials*, **90–93**, 2254–2257.
- Ling, H. I., Wu, J. T. H. & Tatsuoka, F. (1993). Short-term strength and deformation characteristics of geotextiles under typical operational conditions. *Geotextiles and Geomembranes*, **11**, No. 2, 185–219.
- Lins, A. H. P. & Sandroni, S. S. (1994). The development of pore-water pressure in a compacted soil. *International Conference on Soil Mechanics and Foundation Engineering*, New Delhi, India, CRC Press, Boca Raton, FL, USA, pp. 177–180.
- Maher, M. H. & Ho, Y. C. (1994). Mechanical properties of kaolinite fiber soil composite. *Journal of Geotechnical and Geoenvironmental Engineering*, **129**, No. 2, 138–1393.
- Mirzababaei, M., Mirafteb, M., Mohamed, M. & McMahan, P. (2013). Unconfined compression strength of reinforced clays with carpet waste fibers. *Journal of Geotechnical and Geoenvironmental Engineering*, **139**, No. 3, 483–493.
- Nataraj, M. S. & McManis, K. L. (1997). Strength and deformation properties of soils reinforced with fibrillated fibers. *Geosynthetics International*, **4**, No. 1, 65–79.
- NCMA (National Concrete Masonry Association) (2010). *Design Manual for Segmental Retaining Walls*. NCMA, Herndon, VA, USA.
- Nguyen, M. D., Yang, K. H., Lee, S. H., Tsai, M. H. & Wu, C. S. (2013). Behavior of nonwoven-geotextile-reinforced sand and mobilization of reinforcement strain under triaxial compression. *Geosynthetics International*, **20**, No. 3, 207–225.
- Noorzad, R. & Mirmoradi, S. H. (2010). Laboratory evaluation of the behavior of geotextile reinforced clay. *Geotextiles and Geomembranes*, **28**, No. 4, 386–392.
- Parihar, N. S., Shukla, R. P., Gupta, A. K. & Dhawan, S. (2015). Compaction parameters of geotextile reinforced soil. *50th Indian Geotechnical Conference*, Pune, Maharashtra, India.
- Perkins, S. W. (1999). Mechanical response of geosynthetic-reinforced flexible pavements. *Geosynthetics International*, **6**, No. 5, 347–382.
- Plé, O. & Lê, T. N. H. (2012). Effect of polypropylene fiber-reinforcement on the mechanical behavior of silty clay. *Geotextiles and Geomembranes*, **32**, 111–116.
- Portelinha, F. H. M., Bueno, B. S. & Zornberg, J. G. (2013). Performance of nonwoven geotextile-reinforced walls under wetting conditions: laboratory and field investigations. *Geosynthetics International*, **20**, No. 2, 90–104.
- Raisinghani, D. V. & Viswanadham, B. V. S. (2010). Evaluation of permeability characteristics of a geosynthetic-reinforced soil through laboratory tests. *Geotextiles and Geomembranes*, **28**, No. 6, 579–588.
- Ramesh, H. N., Manoj Krishna, K. V. & Mamatha, H. V. (2010). Compaction and strength behaviour of lime-coir fiber treated black cotton soil. *Journal of Geomechanics and Engineering, an International Journal*, **2**, No. 1, 19–28.
- Rollings, M. P. & Rollings, R. R. (1996). *Geotechnical Materials in Construction*. McGraw-Hill, New York.
- Sabat, A. K. & Moharana, R. K. (2015). Effect of compaction energy on engineering properties of fly ash – granite dust stabilized expansive soil. *International Journal of Engineering and Technology*, **7**, No. 5, 1617–1624.
- Soundara, B. & Senthil, K. P. (2015). Effect of fibers on properties of clay. *International Journal of Engineering and Applied Sciences (IJEAS)*, No. 25, 123–128.
- Tan, S. A., Chew, S. H., Ng, C. C., Loh, S. L., Karunaratne, G. P. & Delmas Ph Loke, K. H. (2001). Large-scale drainage behavior of composite geotextile and geogrid in residual soil. *Geotextiles and Geomembranes*, **19**, No. 3, 163–176.
- Tatsuoka, F. & Correia, A. G. (2016). Importance of controlling the degree of saturation in soil compaction. *Procedia Engineering*, **143**, 556–565.
- Tatsuoka, F. & Yamauchi, H. (1986). A reinforcing method for steep clay slopes using a non-woven geotextile. *Geotextiles and Geomembranes*, **4**, No. 3, 241–268.
- Tilak, B. V., Dutta, R. K. & Mohanty, B. (2015). Effect of coir fibres on the compaction and unconfined compressive strength of bentonite-lime-gypsum mixture. *Slovak Journal of Civil Engineering*, **23**, No. 2, 1–8.
- Turnbull, W. J. & Foster, C. R. (1956). Stabilization of materials by compaction. *Journal of the Soil Mechanics and Foundations Division*, **82**, No. 2, 1–23.
- Vinod, P. P., Sridharan, A. & Soumya, R. J. (2015). Effect of compaction energy on CBR and compaction behavior. *Proceedings of the Institution of Civil Engineers-Ground Improvement*, **168**, No. 2, 116–121.
- Walker, J. & Chong, S. K. (1986). Characterization of compacted soil using sorptivity measurements. *Soil Science Society of America Journal*, **50**, No. 2, 288–291.
- Yang, K. H., Yalaw, W. M. & Nguyen, M. D. (2016). Behavior of geotextile-reinforced clay with a coarse material sandwich technique under unconsolidated-undrained triaxial compression. *International Journal of Geomechanics*, **16**, No. 3, 33–45.
- Zornberg, J. G. (2011). Advances in the use of geosynthetic in pavement design. *Proceedings of the Second National Conference on Geosynthetics, Geosynthetics India '11*, India Institute of Technology Madras, Chennai, India, vol. 1, pp. 3–21.
- Zornberg, J. G., Sitar, N. & Mitchell, J. K. (1998). Performance of geosynthetic reinforced slopes at failure. *Journal of Geotechnical and Geoenvironmental Engineering*, **124**, No. 8, 670–683.

The Editor welcomes discussion on all papers published in *Geosynthetics International*. Please email your contribution to discussion@geosynthetics-international.com by 15 August 2020.